ADVANCES IN ATMOSPHERIC SCIENCES, VOL. 31, NOVEMBER 2014, 1305–1315

# Numerical Experiments on the Impact of Spring North Pacific SSTA on NPO and Unusually Cool Summers in Northeast China

LIAN Yi[1,2], ZHAO Bin*[3], SHEN Baizhu[1,2], LI Shangfeng[1,2], and LIU Gang[1,4]

[1]*Laboratory of Research for Middle–High Latitude Circulation Systems and East Asian Monsoon, Changchun* 130062
[2]*Institute of Meteorological Sciences of Jilin Province, Changchun* 130062
[3]*National Meteorological Center, Beijing* 100081
[4]*Jilin Meteorological Science and Technology Service Center, Changchun* 130062

(Received 13 December 2013; revised 11 March 2014; accepted 31 March 2014)

ABSTRACT

A set of numerical experiments designed to analyze the oceanic forcing in spring show that the combined forcing of cold (warm) El Niño (La Niña) phases in the Niño4 region and sea surface temperature anomalies (SSTA) in the westerly drifts region would result in abnormally enhanced NorthEast Cold Vortex (NECV) activities in early summer. In spring, the central equatorial Pacific El Niño phase and westerly drift SSTA forcing would lead to the retreat of non-adiabatic waves, inducing elliptic low-frequency anomalies of tropical air flows. This would enhance the anomalous cyclone–anticyclone–cyclone–anticyclone low-frequency wave train that propagates from the tropics to the extratropics and further to the mid-high latitudes, constituting a major physical mechanism that contributes to the early summer circulation anomalies in the subtropics and in the North Pacific mid-high latitudes. The central equatorial Pacific La Niña forcing in the spring would, on the one hand, induce teleconnection anomalies of high pressure from the Sea of Okhotsk to the Sea of Japan in early summer, and on the other hand indirectly trigger a positive low-frequency East Asia–Pacific teleconnection (EAP) wave train in the lower troposphere.

**Key words**: atmospheric model, westerly drifts, Niño4 SSTA, low-frequency variation, circulation pattern, cool summer, Northeast China

**Citation**: Lian, Y., B. Zhao, B. Z. Shen, S. F. Li, and G. Liu, 2014: Numerical experiments on the impact of spring North Pacific SSTA on NPO and unusually cool summers in Northeast China. *Adv. Atmos. Sci.*, **31**(6), 1305–1315, doi: 10.1007/s00376-014-3247-8.

## 1. Introduction

The concept of the "local circulation pattern" was first introduced in the 1980s and 1990s to represent weather systems that repeatedly appear in a particular region in a sustained or quasi-stationary manner as a result of a remote response to low-frequency oscillation, and to elucidate the forming mechanism of each stage of the circulation pattern (Legras and Ghil, 1985; Mo and Ghil, 1988). Molteni (1993) pointed out that the presence of an extratropical atmospheric flow type does not need the support of SSTA forcing anomalies, though the frequency and stability of a circulation pattern has to be determined by the nature of boundary forcing, including the intensity and sustainability. A study conducted by Bueh and Ji (1999) showed that tropical SSTA may turn a seemingly chaotic tropical atmosphere into a circulation pattern, resulting in partial confinement. Xu et al. (2001) and Xu and Gao (2002) pointed out that blocking is not only an atmospheric nonlinear response to the local forcing, such as a heat source or terrain, but also a result of the nonlinear interactions between fluctuations and local sources (Lu and Huang, 1998; Lu, 2001).

In Northeast China, the influential local circulation patterns are the northeast cold vortex (NECV) and the Asia blocking high. The flow patterns change depending on the presence of internal or external tropical climate systems (Shen et al., 2012; Lian et al., 2013). Liu et al. (2003) revealed that the North Pacific Oscillation (NPO) region's negative 500-hPa height phase in the downstream of Northeast Asia in the winter results in enhanced cold vortex activity in the summer across Northeast China. The enhanced cold vortex activity also produces a climatic effect (He et al., 2006; Liu et al., 2012; Shen et al., 2012). Lian et al. (2010) studied typical northeast cold vortex cases in early summer, and found that the sustained upstream Ural blocking enhances northeast cold vortex activity due to the combined effects of downstream Rossby wave energy dispersion and transient eddy forcing, resulting in precipitation anomalies across the northeastern region (Shen et al., 2011). Numerical experi-

* Corresponding author: ZHAO Bin
Email: zhaob@cma.gov.cn

ments have shown that the North Pacific mid-latitude SSTA in the summer of 1993 could have played a major role in shaping the abnormal southerly position of North Pacific subtropical highs in June and July (Gong et al., 2006). The results, obtained from an improved high spectral model, indicated that the spatial distribution pattern of El Niño's early external thermal forcing created a desirable atmospheric circulation background for the frequent occurrence of Northeast Asian blocking in the summer (Cao et al., 2006).

Lian and An (1998) suggested that El Niño warming events have different OLR (outgoing Longwave Radiation) meridional low-frequency oscillations close to 120°E, depending on whether they originate from the central equatorial or the eastern Pacific. In recent years, researchers have become increasingly interested in understanding the atmospheric response to the central equatorial Pacific SSTA forcing (Ashok et al., 2007; Ratnam et al., 2012; Zhou and Xia, 2012). Lian et al. (2013) performed a diagnosis which found that the unusually cool summers of 1964 and 1993 in Northeast China were supported by an opposite phase configuration of the North Pacific polar vortex, NPO, and North Pacific SSTA in the spring. Though noticeably differing in type, they were equally able to trigger the occurrence of an unusually cool summer in Northeast China. Meanwhile, the northeastern region's early summer temperature has a significant positive correlation with the region's summer temperature as a whole (Li et al., 2012).

In this paper, based on numerical experiments using the CMA3.1 model and experiments on the North Pacific westerly drifts and Niño4 SSTA forcing, we investigate major circulation patterns' responses to SSTA forcing in an attempt to verify the diagnostic conclusion drawn by Lian et al. (2013). We also explore the physical mechanism that allows the low-frequency variation, a response of Niño4 SSTA to the tropical atmospheric warming or cooling in the spring, to propagate to the extratropical region, and its possible impact on the different blocking patterns that could lead to an unusually cool early summer in Northeast China.

## 2. Data and method

The definition of 500-hPa NPO (25°–65°N, 140°E–150°W) and $NPO_L$ index can be found in the literature (Lian et al., 2013), while NECV is defined in the area (35°–60°N, 115°–145°E) where a closed cyclonic circulation at 500 hPa forms and maintains for more than 3 days (Liu et al., 2003). Following the definition of the Okhotsk and Ural blocking highs in East Asia by Liu et al. (2012) (termed the "east" and "west" blockings, respectively, in this paper), the westerly drift index is defined as the normalized area-weighted SSTA in the domain (30°–46°N, 150°E–150°W) (Lian et al., 2013).

In this study, CAM3.1, a 26-level model with a mixed vertical coordinate system developed by National Center for Atmospheric Research (NCAR), is applied. Based on Hadley Center monthly global SST, the standard SST data are taken from the International Comprehensive Ocean-Atmosphere Data Set (ICOADS) and a climatological dataset containing 12 monthly time samples. The monthly mean SSTA forcing is used to define the annual climatic cycle. The North Pacific SSTA variation is defined at a scale of 2°C. The tests are initiated from 1 March with NCAR analysis data. The time step is 1200 s, and the horizontal resolution is chosen as T42 ($128 \times 64$ grid points for the globe). A long-term integration of 50 years is carried out and the last 45 years are selected for analysis.

We (Lian et al., 2013) have pointed out that North Pacific SST in spring and 500-hPa height SVD1 is about 61% of covariance square. The left field is the westerly drifts over North Pacific SST (30°–46°N, 150°E–150°W) and the spatial feature vector is "+". The Niño3.4 spatial feature vector is "−". Matching with the right field 500-hPa height SVD1, in the southern part of $NPO_L$ (25°–45°N, 140°E–150°W), the spatial feature vector is mainly "−" and the northern part of it (50°–65°N, 140°E–150°W) is "+". Therefore, it shows that when the basic mode represents the warm (cold) phase SSTA in the North Pacific and La Nina (El Nino) in Niño3.4, the 500-hPa height over the North Pacific presents a negative (positive) phase $NPO_L$. In this paper, we study in detail the effects of spring $NPO_L$ and cool early summer circulation in Northeast China by westerly drifts and Niño4 SSTA forcing.

Based on the observed results, six numerical sensitivity experiments are designed to analyze the impacts of different combinations of westerly drifts and Niño4 SSTA on northern hemispheric atmospheric circulations, especially their possible impacts on east/west blocking highs and NECV anomalies in Asia that could induce the occurrence of unusually cool summers in Northeast China. The sensitivity experiments are designed as follows:

(1) Experimental regions: region I is a westerly drift region that tilts eastwards (20°–50°N, 170°E–130°W); and region II is a Niño4 region (5°N–5°S, 160°E–150°W) designed to show the effect of central equatorial Pacific SSTA forcing;

(2) Region configurations: region I, Niño4, and region I + Niño4 (see the seven configurations in Table 1).

**Table 1.** Numerical experiments and associated abbreviations.

| Experiment | Definition |
|---|---|
| Control | SST unchanged for 50 years |
| Experiment 1: SUM+2 | Niño4 SST increased by 2°C and westerly drift SSTs decreased by 2°C from March to May for 50 years |
| Experiment 2: SUM-2 | Niño4 SST decreased by 2°C and westerly drift SSTs increased by 2°C from March to May for 50 years |
| Experiment 3: N+2 | Niño4 SST increased by 2°C from March to May for 50 years |
| Experiment 4: N-2 | Niño4 SST decreased by 2°C from March to May for 50 years |
| Experiment 5: X+2 | Westerly drift SSTs increased by 2°C from March to May for 50 years |
| Experiment 6: X-2 | Westerly drift SSTs decreased by 2°C from March to May for 50 years |

## 3. The contribution of spring SSTA forcing to NPO phase patterns

Figure 1a shows that when Niño4 SSTA increases by 2°C and westerly drift SSTA decrease by 2°C, it represents a typical positive NPO phase as a response to atmospheric circulations, where the 500-hPa height anomalies above the Aleutian Islands aligns with those above the subtropics in a north–south "−, +" pattern, constituting a planetary-scale disturbance wave train crossing the North Pacific, with a negative value center up to −120 gpm. A positive value center in the south stretches from the subtropics to the equator and further to the southern hemisphere. On the contrary, when Niño4 SSTA decreases by 2°C and westerly drift SSTA increases by 2°C, a typical negative NPO phase is the response of atmospheric circulations. Consequently, the 500-hPa height anomalies become a strong planetary disturbance wave train crossing the North Pacific in a north–south "+, −" manner from the Aleutians to the subtropics, with a positive value center up to 60 gpm (Fig. 1b).

The combination of Niño4 and westerly drift SSTA shows that the North Pacific atmospheric circulations have a significant positive or negative mode as a response. Here, we also discuss the respective contribution made by Niño4 and westerly drift SSTA to the mode of NPO. Figure 2 presents the 500-hPa height anomalies from experiments 3 and 4 and the control with the presence of El Niño/La Niña SSTA forcing in the Niño4 region. Similarly, the 500-hPa height anomaly fields show two completely different wave train responses from the North Pacific to the North Pole: the 500-hPa height anomaly field has an opposite dipole response in the spring from "−, +" to "+, −". As a result, the scope of the ⩾95% confidence level not only covers most parts of the mid-high latitudes, but also symmetrically covers the entire tropical and subtropical Pacific regions (shaded areas in Figs. 2a and b)—a typical positive or negative NPO phase, suggesting that Niño4 SSTA may result in an NPO teleconnection, which agrees with the previous diagnosis of the positive NPO phase corresponding to the coupled SVD1 mode of El Niño (61% of the total sum of square covariance) (Lian et al., 2013). Previous studies have shown that most PNA-like teleconnections appear in the winter (Van and Rogers, 1981; Van and Madden, 1981). However, the experiments performed in the current study show that a strong spring El Niño SSTA phase in the Niño4 region results in a "+, −, +" wave train from the North Pacific to the Bering Strait, and further to northwestern Canada, suggesting that the warm central equatorial Pacific SSTA forcing in the spring produces a PNA-like teleconnec-

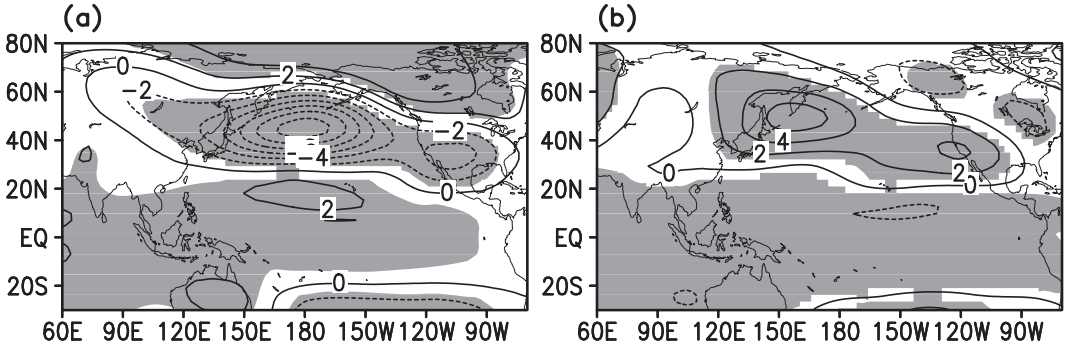


**Fig. 1.** 500-hPa height anomalies of Experiment (1 and 2) and the control, (a) Experiment 1, (b) Experiment 2. The shaded areas are the one that have passed the 95% confidence level, with the thin solid lines for the 500-hPa positive geopotential anomalies and the thin dashed lines for the 500-hPa negative geopotential anomalies in geopotential meter.

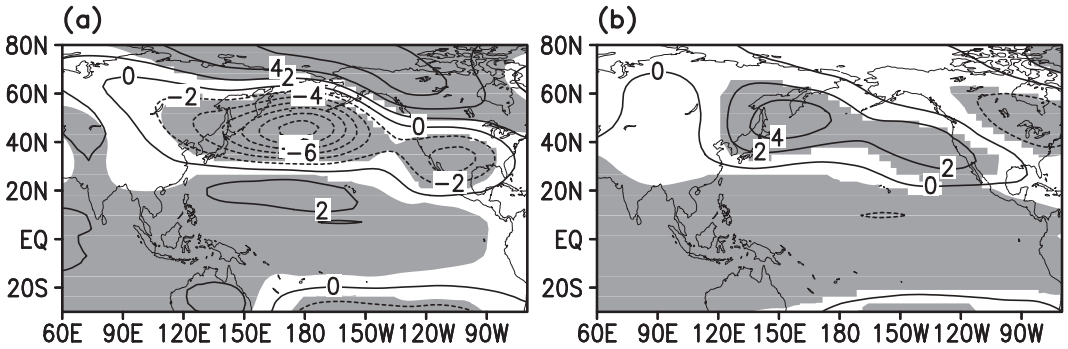


**Fig. 2.** 500-hPa height anomalies of Experiment (1 and 2) and the control, (a) Experiment 3, (b) Experiment 4. The shaded areas are the one that have passed the 95% confidence level, with the thin solid lines for the 500-hPa positive geopotential anomalies and the thin dashed lines for the 500-hPa negative geopotential anomalies in geopotential meter.

tion as a response to atmospheric circulations.

The results derived from experiments 3 and 4 and the control are quite similar to those from experiments 1 and 2, albeit with a 10-gpm difference (Figs. 2a, b and Figs. 1a, b), which fully agrees with the fact that El Niño's (La Niña's) positive (negative) NPO phase in the Niño4 region is the most significant forcing source contributing to a positive or negative NPO phase.

Figure 3 shows the 500-hPa height anomalies of experiment 6 and the control, where a planetary-scale negative anomaly belt stretches from Balkhash Lake to the Sea of Okhotsk and further to the Aleutians, with a negative anomaly center located in the south of the Aleutians, supported by a value center of $<25$ gpm. The whole of Northeast Asia and the Aleutians show significant anomalies ($\geqslant$95%). There is a weak positive anomaly region above the mid-latitudes and the subtropics, with a north–south "$-$, $+$" wave train above the North Pacific and the Aleutians, suggesting a typical positive NPO phase. The significant positive anomaly region ($\geqslant$95%) stretches from eastern Siberia to the northern part of the Sea of Okhotsk and further to Alaska, constituting a north–south "$+$, $-$" dipole circulation pattern together with the negative anomalies in the south of the Aleutians. In the west stands a typical Northeast Asian blocking made up of the Sea of Okhotsk high and NECV. Unfortunately, the pattern, as such, only appears in the spring rather than in early summer. In addition, the 500-hPa height anomalies of experiment 5 and the control, in which westerly drifts are given an increase of temperature by 2°C, failed to show the negative NPO phase (figure omitted).

The simulation results of Niño4 SSTA forcing is consistent with the atmospheric results from the combination of Niño4 and westerly drift SSTA forcing, except that the positive NPO phase forced out by El Niño has a North Pacific anomaly center that is smaller in magnitude compared with the combined anomalies, and that the circulation pattern derived from La Niño has an anomaly magnitude that is equivalent to the one from the combined anomalies. Cold SSTA contributes to westerly drift forcing. The magnitude of anomaly becomes larger when the modal anomaly is added to the Niño4 SSTA forcing anomaly, with a result closer to the combined anomalies, suggesting a major contribution of Niño4 to a positive NPO phase. Cold westerly drift SSTA contributes to an enhanced positive NPO phase. Meanwhile, it is only Niño4 SSTA, rather than westerly drift SSTA, that contributes to a negative NPO phase.

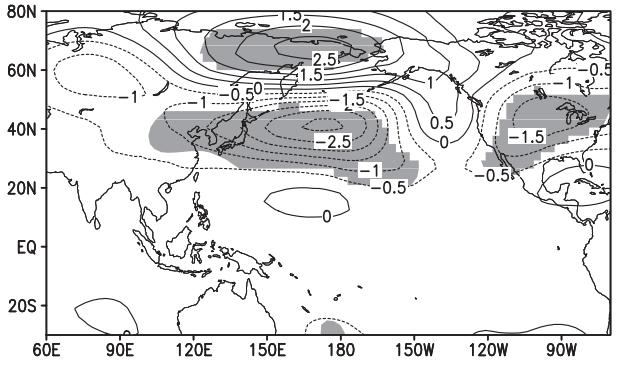


**Fig. 3.** 500-hPa height anomalies of Experiment 6 and the control. The shaded areas are the one that have passed the 95% confidence level, with the thin solid lines for the 500-hPa positive geopotential anomalies and the thin dashed lines for the 500-hPa negative geopotential anomalies in geopotential meter.

## 4. Impact of spring SSTA forcing on early summer atmospheric circulation anomalies in Northeast Asia

As reported above, the impact of the combined forcing of Niño4 and westerly drift SSTA on NPO phases has been analyzed. In this section, we investigate the role played by a non-adiabatic NPO, arising from the joint effects of sea surface temperature and atmosphere (Chou, 1986), in inducing a retreating wave that could lead to early summer blocking abnormalities across Northeast Asia, and the physical process that would trigger an unusually cool early summer in Northeast China.

### 4.1. *Combined forcing of warm Niño4 and cold westerly drifts encourages NECV activities in early summer*

Figure 4 presents the 500-hPa height anomalies of experiment 1 and the control. In March, it shows a negative anomaly center stretching from Northeast Asia to the Aleutians, with a central value of up to 80 gpm. There is a negative anomaly center that covers some areas in the central and southern part of North America. Meanwhile, significant anomalies cover most parts of the region. There is an extensive positive anomaly corridor distributed from the East Siberian Sea in the north of the Aleutians to Alaska and further to northwestern Canada, with significant anomalies covering most parts of the region, conducive for Polar ridge activities. A weak height anomaly region can be seen over the central subtropical and tropical Pacific in the south of the Aleutians, although an impressive part of the region passed the $\geqslant$95% confidence level (Fig. 4a). April–May shows a peak anomaly that runs north–south in a "$+$, $-$, $+$" manner, forcing out the westbound retreat of the negative anomaly center above the Aleutians by some 30° of longitude (Figs. 4b and c). In May, the largest negative anomaly reaches $\leqslant -120$ gpm above the Aleutians, with a further expanded domain of $\geqslant$95% confidence (Figs. 4c and a). In June, the north–south "$+$, $-$" anomaly wave train is sustained over a vast region from the North Pole to the North Pacific high latitudes, albeit with a noticeably weakened strength. Whereas, the negative value region remains able to stretch westwards to Northeast Asia and even to central Asia, with a negative anomaly of up to $-40$ gpm across Northeast Asia (Fig. 4d).

Experiment 1 shows that the combined forcing of warm Niño4 and cold westerly drifts would have a lasting impact on the presence of a positive NPO phase, and that the significant westbound retreat of negative Aleutian anomalies in the positive NPO phase would encourage early summer NECV activ-

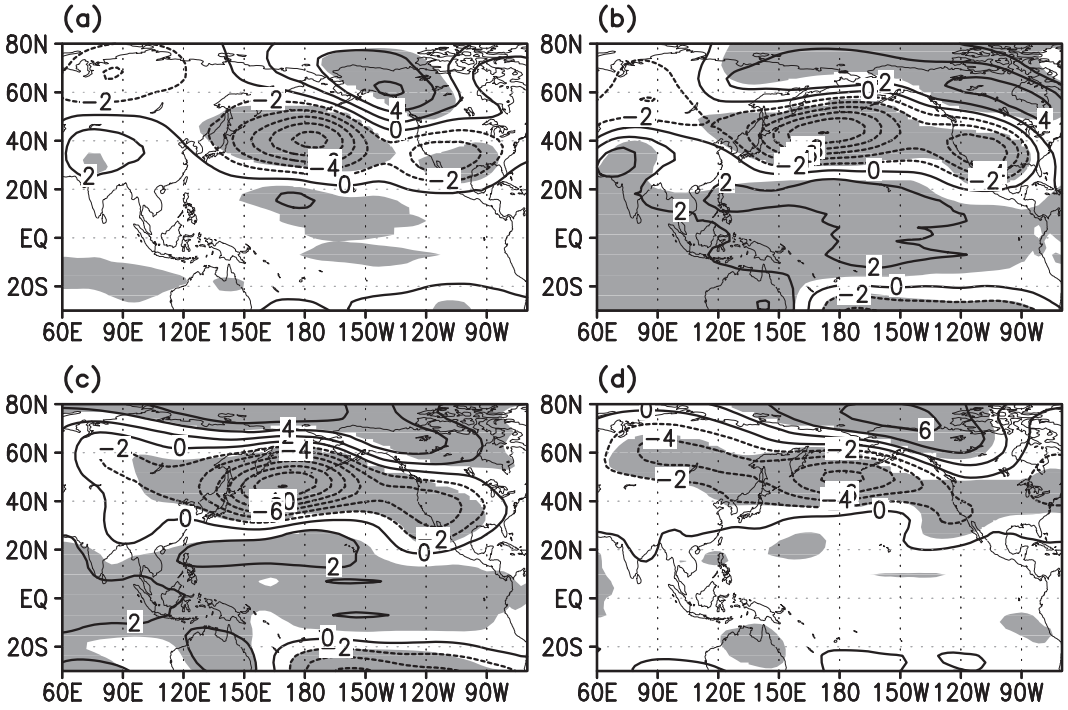


**Fig. 4.** 500-hPa height anomalies of Experiment 1 and the control (a) March, (b) April, (c) May, and (d) June. The shaded areas are the one that have passed the 95% confidence level, with the thin solid lines for the 500-hPa positive geopotential anomalies, and the thin dashed lines for the 500-hPa negative geopotential anomalies in geopotential meter.

ities in Northeast Asia, which is quite similar to the physical process that staged an NECV circulation pattern in the early summer of 1993 across Northeast Asia that led to an unusually cool summer in Northeast China (Lian et al., 2013).

### 4.2. *Cold Niño4 SSTA and warm westerly drifts encourage positive Okhotsk high anomalies*

Figure 5 shows the 500-hPa height anomalies of experiment 2 and the control. It indicates that during the period of March–May, the 500-hPa height field responds to the broad symmetric negative anomaly belt, with the equator as the axis, in the subtropical regions of both the northern and southern hemispheres, with the largest negative anomaly at $\leqslant -20$ gpm in May. The significant anomalies ($\geqslant$95%) basically envelope the entire region, suggesting southerly and easterly subtropical high activities (Figs. 5a–c). In April–May, the positive anomaly center stretches into a planetary-scale belt from the Sea of Okhotsk to the west coast of the United States, with the central value in the south of the Sea of Okhotsk of up to 80 gpm. Significant anomalies ($\geqslant$95%) cover the entire region, supporting a stable and sustained negative NPO phase (Figs. 5b and c). In June, the negative NPO anomaly center becomes noticeably weakened, although remains over a region from the Sea of Okhotsk to the Sea of Japan ($\geqslant$95%), constituting a "low in the west and high in the east" dipole circulation pattern together with the relatively weak negative anomalies that flank Lake Baikal in the west.

Experiment 2 produces a combined forcing of cold Niño4 and warm westerly drifts that encourage the formation of a negative NPO phase. Meanwhile, the stationary wave of positive anomalies in the negative NPO phase makes a significant contribution to the early summer positive anomalies of the Sea of Okhotsk, bearing some similarity to the eastern blocking that prevailed across Northeast Asia in the summer of 1964, where a severe unusually cool summer was reported in Northeast China (Lian et al., 2013).

### 4.3. *Niño4 La Niña and El Niño encourage high anomalies in the south of Okhotsk and low anomalies in the northeast*

Figure 6 shows the 500-hPa height anomalies of June from experiments 3 and 4 featured with La Niña SSTA and El Niño SSTA forcing in the Niño4 region. Two completely different responses can be seen at 500 hPa in early summer. Under the thermal forcing of El Niño ($+2^{\circ}$C), significant early summer negative anomalies appear as a response over the mid-high latitudes, from the central Pacific subtropics to the Aleutians, Alaska, and further to the North Atlantic in the north, in a "+, −, +" wave train pattern, with the latter two (−, +) being stronger, suggesting that El Niño encourages low-pressure activities in East Asia, the Aleutians, and the central and northern parts of the United States, with the $\geqslant$95% confidence level covering the entire region. Additionally, there is a weak positive anomaly region above the Ural Mountains, albeit at a poor confidence level. It produces a "high in the west and low in the east" pattern similar to the circulation pattern that prevailed in the summer of 1964, where an unusually severe cool summer occurred in North-

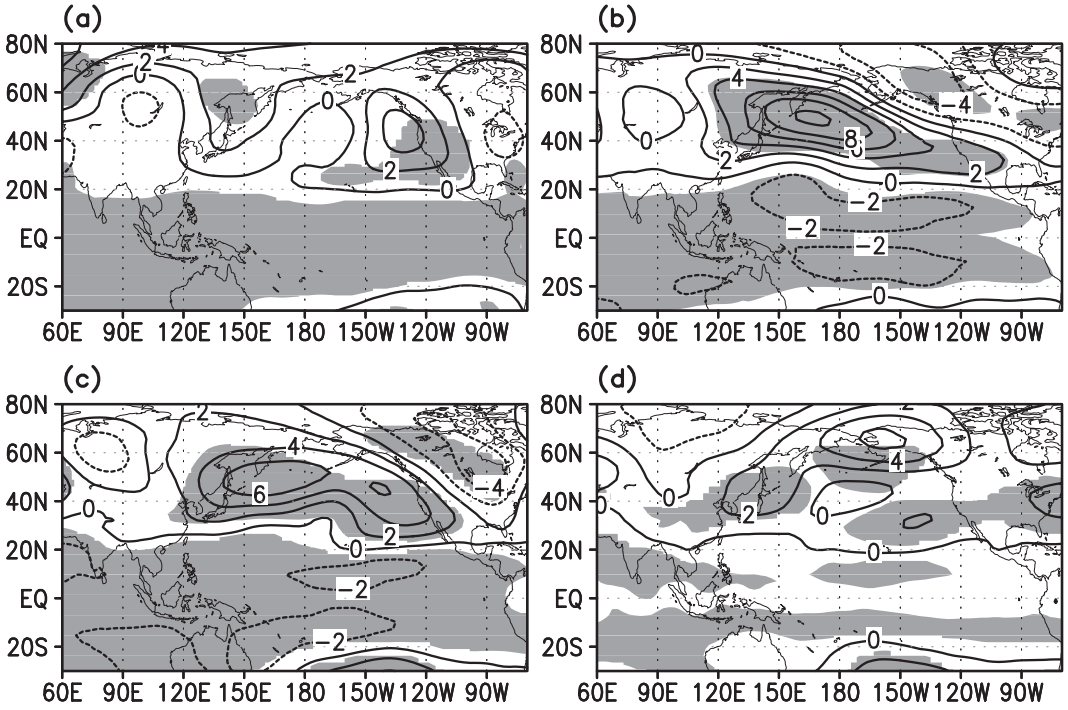


**Fig. 5.** 500-hPa height anomalies of Experiment 2 and the control (a) March, (b) April, (c) May, and (d) June. The shaded areas are the one that have passed the 95% confidence level, with the thin solid lines for the 500-hPa positive geopotential anomalies and the thin dashed lines for the 500-hPa negative geopotential anomalies in geopotential meter.

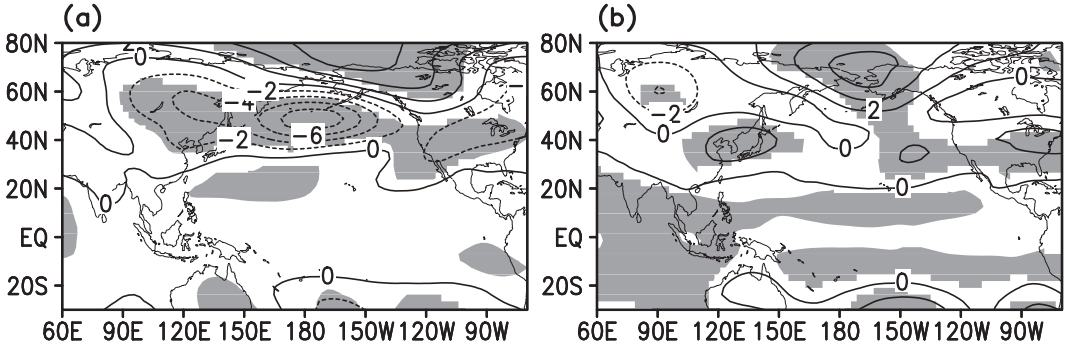


**Fig. 6.** 500-hPa height anomalies of Experiments (3 and 4) and the control in June, (a) Experiment 3, (b) Experiment 4. The shaded areas are the one that have passed the 95% confidence level, with the thin solid lines for the 500-hPa positive geopotential anomalies and the thin dashed lines for the 500-hPa negative geopotential anomalies in geopotential meter.

east China (Fig. 6a; Lian et al., 2013). The thermal forcing of cold Niño4 SSTA (La Niña −2°C) results in a significant positive anomaly in the south of the Sea of Okhotsk, including Northeast China, suggesting that cold Niño4 SSTA is desirable for the maintenance and development of southerly eastern blocking. Meanwhile, there is a relatively weak negative anomaly region in the west of Lake Baikal. There is also a relatively strong positive anomaly belt from the East Siberian Sea to Alaska. The positive anomaly belt from the Northeast Pacific to the central and eastern parts of the United States is as strong as the one in the south of the Sea of Okhotsk, with a ⩾95% confidence level covering the entire region (Fig. 6b).

The results from experiments 3 and 4 (Figs. 6a and b) are very similar to those from experiments 1 and 2 (Figs. 4d and 5d), suggesting that El Niño or La Niña forcing in the Niño4 region plays a dominant role in shaping the major North Pacific SSTA phases.

### 4.4. *Weak impact of cold/warm westerly drift forcing on East Asian blocking*

Figure 7 shows the 500-hPa height anomalies of Experiment 6 and the control with a decreased (by 2°C) westerly drift SSTA from March to May. The results show that a planetary-scale 500-hPa positive anomaly belt stretches from

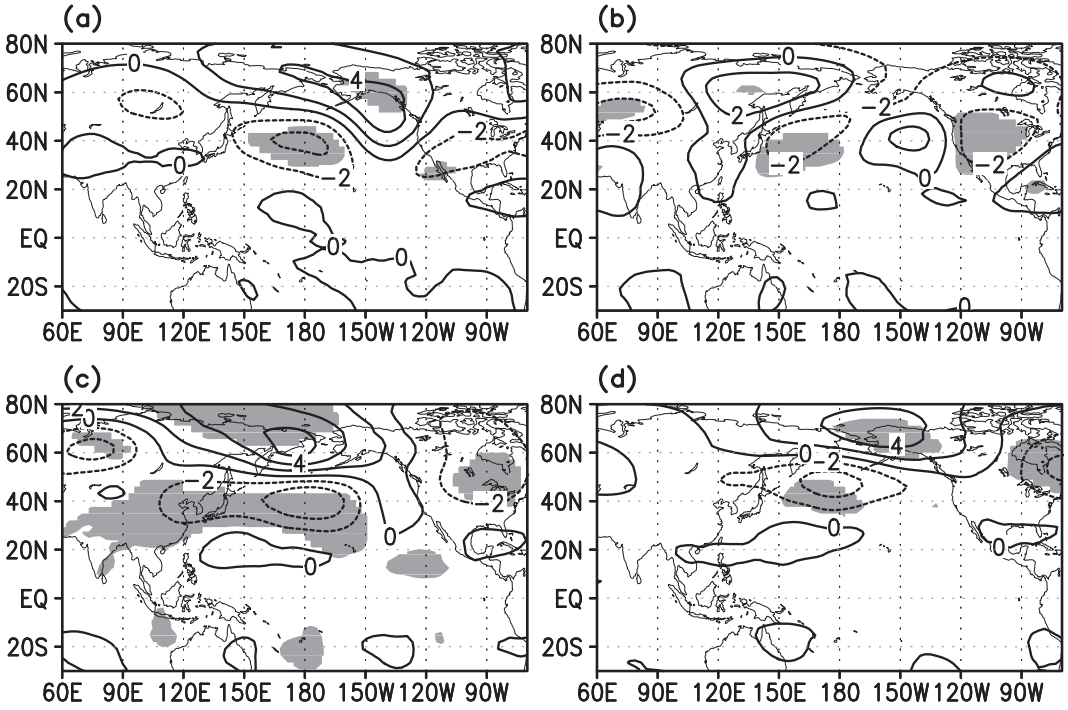


**Fig. 7.** 500-hPa height anomalies of Experiment 6 and the control (a) March, (b) April, (c) May, and (d) June. The shaded areas are the one that have passed the 95% confidence level, with the thin solid lines for the 500-hPa positive geopotential anomalies and the thin dashed lines for the 500-hPa negative geopotential anomalies in geopotential meter.

eastern Siberia to Alaska throughout March–May with a confidence level up to $\geqslant$95%. Meanwhile, there is a planetary-scale negative anomaly belt in East Asia from the Sea of Japan to the Aleutians, constituting a "+, −" wave train from the polar region to Northeast Asia and further to the Aleutians, supported by $\geqslant$95% confidence. In addition, there is an unstable negative anomaly region above the North American continent (Figs. 7a–c). In June, the 500-hPa height anomaly field, despite a "+, −" wave train remaining over the polar region and the Pacific Ocean, becomes noticeably weakened and shrinks eastwards, compared with the strongest "+, −" wave train appearing in May from the polar region to Northeast Asia and further to the Aleutians, suggesting that the cold westerly drift forcing in the spring would have an impact on NECV anomalies that would be strong in May but weak in early summer. In early summer, it only has an effect on the "+, −" wave train from the polar region to the North Pacific. The 500-hPa height anomalies of Experiment 5 and the control, with a westerly drift SSTA increased by 2°C from March to May, show that there is neither a stationary anomaly wave train nor the support of $\geqslant$95% confidence (figure omitted).

## 5. Physical mechanism underpinning the Niño4 forcing and low-frequency atmospheric response

In this section we analyze the 850-hPa tropical and extratropical low-frequency variation pattern induced by sustained Niño4 SSTA forcing (+2°C or −2°C) from March to June, and explain the possible physical mechanisms that produce the numerical experiment results described in the previous two sections through the effect of energy dispersion. In doing so we hope to facilitate a comparison of the results with those from other major national and international numerical experiment studies.

### 5.1. *Elliptic extratropical low-frequency variation pattern induced by El Niño makes the "C–A–C–A" low-frequency wave train more significant*

Figure 8 shows the evolution of 850-hPa flow fields from experiment 3 and the control from March to June. In March, it is under the influence of strong cold surges sweeping over China's eastern coasts and the west Pacific warm pool around the Philippines (see Fig. 8a, in which strong northwesterly flow anomalies can be seen spreading from the west of Lake Baikal to China's east coast and further to the central Pacific, before forming a closed anticyclonic flow anomaly field in the north of the Philippines, as shown in the north of the black box). The 850-hPa Niño4 flow anomaly field in the central tropical equator sits in a symmetric parabolic low-frequency variation pattern with the equator as the axis (see the square area in Fig. 8a that tracks the flow anomaly variations in other months). With an SSTA increased by 2°C in April, a literally closed cyclonic low-frequency circulation pattern appears in the north of the central equatorial Pacific Niño4 region. Meanwhile, the subtropical area at 20°N quickly forms a closed anticyclonic circulation pattern, which enhances the

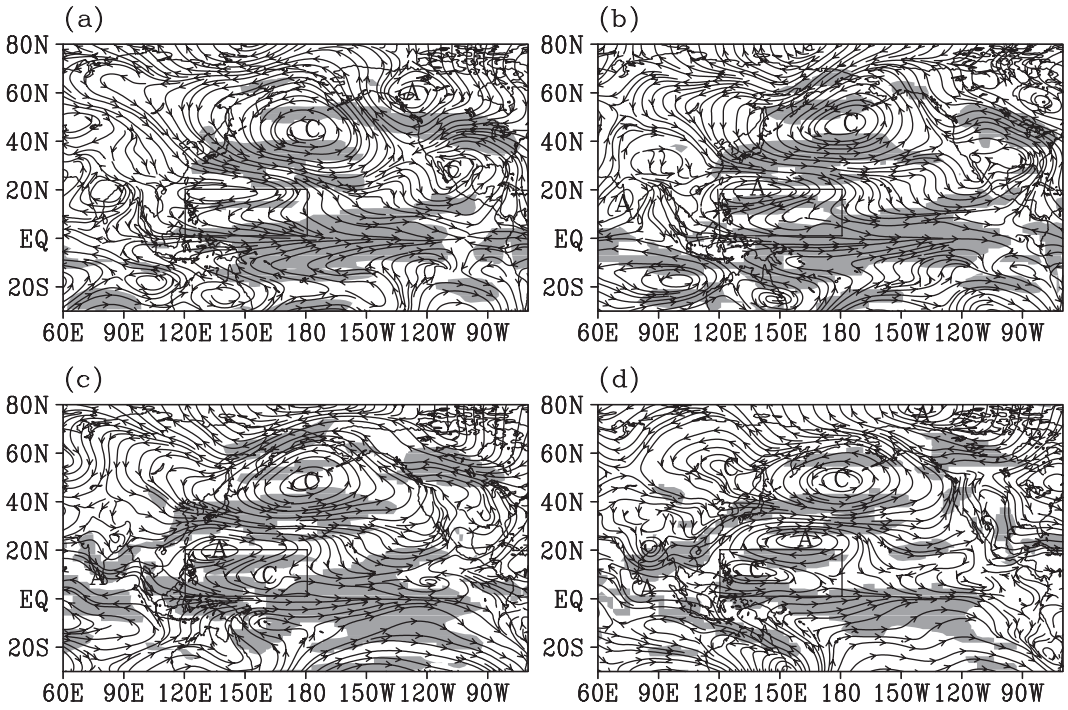


**Fig. 8.** 850-hPa flow anomalies of Experiment 3 and the control from March to June, (a) March, (b) April, (c) May, and (d) June. The shaded areas are the one that have passed the 95% confidence level, with the thin solid lines for the 850-hPa flow lines.

cyclonic circulation that has been sustained above the Aleutians since March (compare Figs. 8a and b). In May, a significant cyclonic flow pattern appears in the northern part of the central equatorial Pacific Niño4 region, with an enhanced anticyclonic flow pattern in the northwest of the subtropics. As a result, the cyclonic flows above the Aleutians prevail over the North Pacific mid-high latitudes, with their westbound retreating center joining the cyclonic flows in the west of Lake Baikal. The evolution leaves no intact anticyclonic circulation above the Sea of Okhotsk. In the spring NPO sits in a positive phase, overseeing the northeast–southwest presence of cyclone (C) and anti-cyclonic (A) over the North Pacific. The 850-hPa flow anomaly field of Experiment 3 and the control in June shows that an intact elliptical low-frequency cyclonic circulation pattern appears above the tropical ocean east of the Philippines (the black box in Fig. 8d). Meanwhile, the northeast bound subtropical anticyclone moves northwards by 5° of latitude and eastwards by 30° of longitude (compare Figs. 8c and d), before traveling through the powerful Aleutian low-frequency cycle and the Arctic anticyclone in northern Alaska, forming a "C–A–C–A" low-frequency wave train (Fig. 8d). In addition, the westbound expansion of the Aleutian low-frequency cyclone "C" results in another cyclonic circulation center ("C") over Northeast Asia, encouraging NECV activities. Both the easterly and westerly flow anomalies in the southern and northern flanks of each wave train center reach the $\geqslant$95% confidence level (Fig. 8).

The evolution of 850-hPa flow anomalies in Experiment 3 and the control from March to June show that, under the strong influence of non-adiabatic and regional divergence flows stemming from the mid-latitudes, the tropical region would see a parabolic low-frequency variation pattern (Fig. 8a). When the warm tropical SSTA disturbance exceeds the influence of non-adiabatic and regional divergence flows in April–May, there would be a full elliptical low-frequency cyclonic circulation variation pattern over the central and west part of the tropical Pacific. This, under the effect of energy dispersion, would reinforce the southwest–northeast C–A–C–A low-frequency variation wave train that travels from the tropics to the subtropics, and further to the mid-high latitudes (Fig. 8d). This explains the physical mechanism that allows the warm spring Niño4 SSTA forcing to encourage the presence of positive NPO anomalies, which would in turn significantly weaken the Okhotsk blocking high (east blocking) in early summer.

### 5.2. *La Niña contributes to a positive low-frequency EAP wave train*

Figure 9 shows the 850-hPa flow anomalies of experiment 4 and the control from March to June. It indicates a symmetric parabolic low-frequency variation pattern, with the equator as the axis, during that period (the square area in Fig. 9a), without sending waves to the extratropical high latitudes of the Northern Hemisphere. This constitutes a substantive difference from the elliptic pattern derived from experiment 3, in which the La Niña phase in the Niño4 region shows a parabola, dual-curve and straight trajectory without tropical non-adiabatic heating (Xu and Gao, 2002). In June, a "C–A–C–A–C" wave train forms along Asian east coasts, travel-

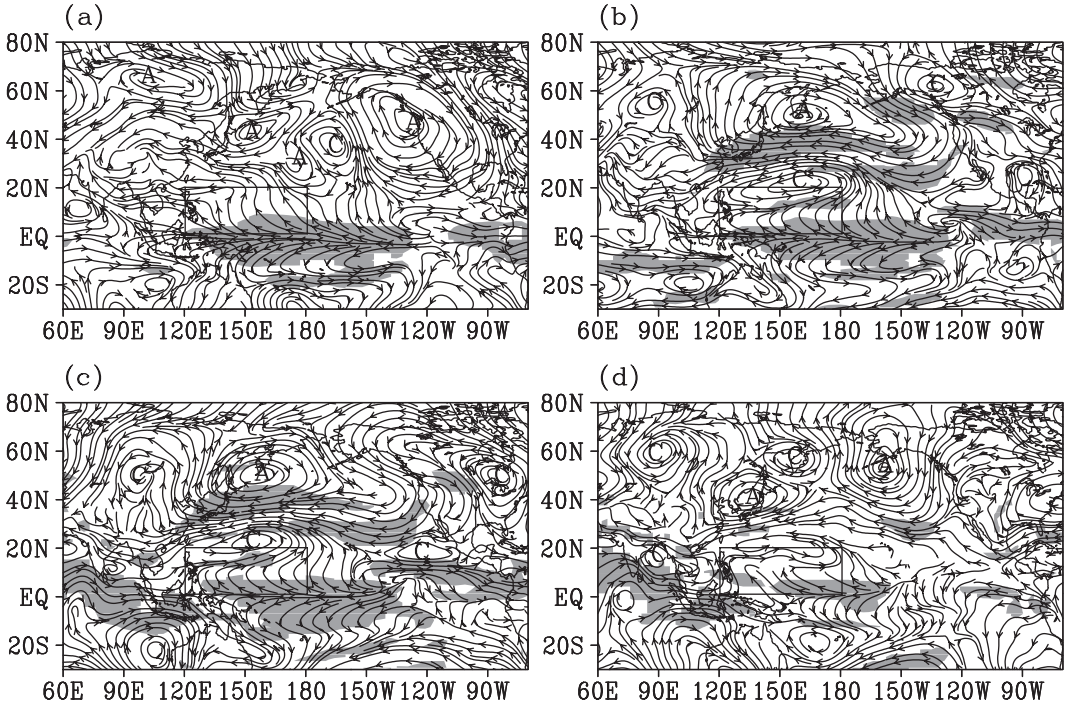


**Fig. 9.** 850-hPa flow anomalies of Experiment 4 and the control from March to June (a) March, (b) April, (c) May, and (d) June. The shaded areas are the one that have passed the 95% confidence level, with the thin solid lines for the 850-hPa flow lines.

ing across the western Pacific warm pool, China's east coast, Japan's Honshu Island, the Aleutians, and America, becoming a typical positive EAP phase, which is obviously associated with the indirect thermal forcing of the western Pacific warm pool in the Niño4 region with an SSTA decreased by 2°C (Nitta, 1987; Huang and Li, 1987). The westerly and easterly anomalies above the western Pacific warm pool and the subtropical region register a confidence level of $\geqslant$95% (Fig. 9d).

## 6. Summary and discussion

The combined results from the numerical sensitivity experiments (1–4) conducted in this study provide further evidence that two different modal forcing of El Niño (La Niña) and cold (warm) westerly drifts in the Niño4 region would have a positive (negative) NPO phase as an atmospheric response over the North Pacific in spring. Hereon, SST forcing over the Niño4 region presents a major contribution to the NPO positive (negative) phase modal the westerly drift SSTA forcing shows obviously asymmetry in response to mid-high latitude circulation, and only cold SST forcing contributes to strengthening the NPO positive phase modal; while the NPO negative phase modal only depends on the Niño4 region SST, regardless of the westerly drift. The Niño4 region SST forcing in the North Pacific is far more important than SSTA of the westerly drift from the perspective of ocean forcing, this provides further evidence of a sea–air coupled mode over the North Pacific in the spring. It also confirms that these two major coupled modes can serve as precursor signals for the commencement of an unusually cool summer in Northeast China (Lian et al., 2013).

The results of experiment 1 and the control, featuring a warm Niño4 and cold westerly drifts, show that this combination would lead to a significant westbound retreat of the non-adiabatic positive NPO phase, rendering a significant contribution to the enhanced early summer NECV activities at 500 hPa. This is similar to the major configurations of the North Pacific SSTA pattern and NECV circulation pattern that prevailed in Northeast Asia in the early summer of 1993, and that encouraged the occurrence of an unusually cool early summer in Northeast China (Lian et al., 2013). Experiment 2, designed with a combination of cold Niño4 and warm westerly drifts, shows that the non-adiabatic positive NPO phase anomaly center, jointly formed by SSTA and the atmosphere in the spring, would allow the stationary wave to make a significant contribution to the positive anomalies in the region from the Sea of Okhotsk to the Sea of Japan. This bears a resemblance to the major North Pacific SSTA configurations in the spring of 1964, and to the eastern blocking that also prevailed over Northeast Asia in the summer of that same year (Lian et al., 2013).

Experiments 3 and 4 and the control produced a range of results that are very similar to those derived from the combination of experiments 1 and 2, suggesting that El Niño/La Niña forcing in the Niño4 region may play a dominant role in shaping the major North Pacific SSTA modes, although the impact on the Ural High anomalies in early summer would be insignificant. The circulation pattern forced out by La Niña would have a magnitude that matches the combined phase

anomalies. Meanwhile, experiments 5 and 6 and the control produced a result showing that only cold westerly drift forcings would have a significant impact. The anomaly would become larger in magnitude, if the mode anomaly is added to the Niño4 SSTA forcing anomaly, making it closer to the combined anomalies.

A reasonable explanation for the above-mentioned results is found in the 850-hPa flow anomalies stemming from experiments 3 and 4 and the control from March to June. When the warm central equatorial Pacific Niño4 SSTA disturbance exceeds the non-adiabatic influence from the mid-latitudes, there would be a full elliptical low-frequency cyclonic variation in the region, reinforcing the C–A–C–A low-frequency variation wave train ($\geqslant$95%). The significant westbound retreat of "C" above the Aleutians would result in a new cyclonic circulation center, "C", encouraging the early summer NECV activities in the northeast. The cold central equatorial Pacific SSTA forcing would see a parabolic or linear low-frequency variation pattern. Although not directly triggering the northward propagation of the low-frequency wave train, the pattern, as such, would indirectly trigger a positive EAP wave train in early summer (June), due to the fact that the cold central equatorial Pacific phase would remain an obvious heat source compared with the western Pacific warm pool. Such a wave train pattern would encourage cyclonic circulations above the Sea of Okhotsk, albeit with a weak strength at a poor confidence level. As a result, the central equatorial Pacific La Niña forcing would encourage abnormal high pressure activities in the south of Okhotsk in early summer, which supports the theoretical results on tropical low-frequency oscillation trajectories using the WKBJ method (Xu et al., 2001; Xu and Gao, 2002). It confirms the conclusion drawn in the study by Lim and Chang (1983), and reveals the low-frequency variation of different phase trajectories, including cold and warm central equatorial Pacific SSTA forcing, which would in turn help determine if there is a low-frequency variation wave train between the tropical, subtropical and mid-high latitudes.

In Northeast China, the early summer temperature has a strong correlation with the summer temperature as a whole. In this context, the classified extraction and integration of the early signals that would foresee an unusually cool early summer plays a pivotal role in the short-term prediction of the early summer temperatures of Northeast China.

The two spring precursor signals that foretell an unusually cool summer in Northeast China would have an opposite sea–air configuration in the North Pacific. This study has presented a reasonable explanation through a range of numerical experiments: in the spring, the different combinations of North Pacific westerly drifts and Niño4 SSTA forcing would result in a different positive or negative NPO phase. The different sea–air coupling configurations would make a noticeable difference to the early summer blocking anomalies prevailing in Northeast Asia. The paper has also discussed the low-frequency variation process triggered by the central equatorial Pacific SSTA thermal forcing, and the physical mechanisms underpinning the mid-high latitude circulation anomalies. Another major mechanism that may also have an impact on the occurrence of unusually cool summers in Northeast China, or the Ural blocking, may involve forcings derived from other oceans, which requires further investigation in a separate paper.

***Acknowledgements.*** This study was supported by a National Natural Science Foundation project approved under Grant Nos. 41175083, 41275096 and 41305091, and a China Meteorological Administration special public welfare reserch funds registered under Grant Nos. GYHY201006020, GYHY 201106016, and GYHY201106015.

## REFERENCES

Ashok, K., S. K. Behera, S. A. Rao, H. Weng, and T. Yamagata, 2007: El Niño Modoki and its possible teleconnection. *J. Geophys. Res.*, **112**, C11007, doi: 10.1029/2006JC003798.

Bueh, C. L., and L. R. Ji, 1999: The ocean–atmosphere coupled regimes and east Asian winter monsoon (EAWM) activity. *Adv. Atmos. Sci.*, **16**, 91–106, doi: 10.1007/s00376-999-0006-3.

Cao, J., R. H. Huang, and Y. Tao, 2006: A mechanism for interannual variations of Northeast Asian Blocking High in summer. *Chinese J. Geophys.*, **49**, 37–44. (in Chinese)

Chou, J. F., 1986: *Long Range Numerical Weather Forecast*. China Meteorological Press, Beijing, 329 pp. (in Chinese)

Gong, Y. F., J. H. He, T. Y. Duan, and P. Pan, 2006: Numerical experiment on the influences of minus-ssta over mid-latitude northern Pacific on the subtropical anticyclone. *Journal of Tropical Meteorology*, **22**, 386–392. (in Chinese)

He, J. H., Z. W. Wu, Z. J. Hong, C. S. Miao, and G. R. Han, 2006: Climate effects of northeast cold vortex and its impacts on plum rains. *Chinese Science Bulletin*, **5**, 2803–2809. (in Chinese)

Huang, R. H., and W. J. Li, 1987: Influence of the heat source anomaly over the western tropical Pacific on the subtropical high over East Asia. *Proc. International Conference on the General Circulation of East Asia*, April 10–15, Chengdu, 40–51.

Legras, B., and M. Ghil, 1985: Persistent anomalies, blocking and variations in atmospheric predictability. *J. Atmos. Sci.*, **42**, 433–471.

Li, S. F., Y. Lian, S. B. Chen, Q. H. Sun, and Y. X. Yao, 2012: Distribution of extreme cool events over Northeast China in early summer and the related dynamical processes. *Scientia Geographica Sinica*, **32**, 752–758. (in Chinese)

Lian, Y., and G. An, 1998: The relationship among East Asia summer monsoon, El Niño and low temperature in Songliao plains Northeast China. *Acta Meteorologica Sinica*, **56**, 724–735. (in Chinese)

Lian, Y., C. L. Bueh, Z. W. Xie, and F. S. Li, 2010: The anomalous cold vortex activity in Northeast China during the early summer and the low-frequency variability of the northern hemispheric atmosphere circulation. *Chinese J. Atmos. Sci.*, **34**, 429–439. (in Chinese)

Lian, Y., B. Z. Shen, S. F. Li, B. Zhao, Z. T. Gao, G. Liu, P. Liu, and L. Cao, 2013: Impacts of polar vortex, NPO, and SST configurations on unusually cool summers in Northeast China. Part I: Analysis and diagnosis. *Adv. Atmos. Sci.*, **30**, 193–209, doi:

10.1007/s00376-012-1258-x.

Lim, H., and C.-P. Chang, 1983: Dynamics of teleconnections and Walker circulations forced by equatorial heating. *J. Atmos. Sci*., **40**, 1897–1915.

Liu, G., B. Z. Shen, Y. Lian, S. F. Li, L. Cao, and P. Liu, 2012: The sorts of 500hPa blocking high in Asia and it's relations to cold vortex and aestival low temperature in Northeast of China. *Scientia Geographica Sinica*, **32**, 1269–1274. (in Chinese)

Liu, Z. X., Y. Lian, B. Z. Shen, Z. T. Gao, and X. L. Tang, 2003: Variation features of 500hPa height in north pacific oscillation region and its effect on precipitation in Northeast China. *Journal of Applied Meteorological Science*, **14**, 553–561. (in Chinese)

Lu, R. Y., 2001: Eddies during the blocking maintenance over the Northeastern Asia in summer. *Chinese J. Atmos. Sci*., **25**, 289–302. (in Chinese)

Lu, R. Y., and R. H. Huang, 1998: Influence of East Asia/Pacific teleconnection pattern on the interannual variations of the blocking highs over the Northeastern Asia in summer. *Chinese J. Atmos. Sci*., **22**, 727–734. (in Chinese)

Mo, K. C., and M. Ghil, 1988: Cluster analysis of multiple planetary flow regimes. *J. Geophys. Res*., **93**, 10 927–10 951.

Molteni, 1993: Research activities in atmospheric and oceanic modelling. CAS/JSC Working Group Numerical Experimentation. Geneva, Switzerland, WMO.

Nitta, T., 1987: Convective activities in the tropical western Pacific and their impact on the Northern Hemisphere summer circulation. *J. Meteor. Soc. Japan*, **65**, 373–390.

Ratnam, J. V., S. K. Behera, Y. Masumoto, K. Takahashi, and T. Yamagata, 2012: Anomalous climatic conditions associated with the El Niño Modoki during boreal winter of 2009. *Climate Dyn.*, **39**, 227–238.

Shen, B. Z., Z. D. Lin, R. Y. Lu, and Y. Lian, 2011: Circulation anomalies associated with interannual variation of early-and late-summer precipitation in Northeast China. *Science China Earth Sciences*, **54**, 1095–1104.

Shen, B. Z., S. Liu, Y. Lian, G. L. Feng, S. F. Li, and Z. Q. Gong, 2012: The 2009 summer low temperature in Northeast China and its association with prophase changes of the air–sea system. *Acta Meteorologica Sinica*, **26**, 320–333.

Van, L. H., and R. A. Madden, 1981: The southern oscillation, Part I: Global associations with Pressure and temperature in northern winter. *Mon. Wea. Rev.*, **109**, 1150–1162.

Van, L. H., and J. C. Rogers, 1981: The southern oscillation, Part II: Associations with changes in the middle troposphere in the northern winter. *Mon. Wea. Rev.*, **109**, 1163–1168.

Xu, X. D., and Coauthors, 2001: Comprehensive physical picture of dynamic and thermal structure in Qinghai-Tibet Plateau. *Science in China* (*D*), **31**, 428–440. (in Chinese)

Xu, X. D., and S. T. Gao, 2002: *Dynamics of External Forcing and Wave-Current Interaction*. China Ocean Press, Beijing, 291 pp. (in Chinese)

Zhou, B. T., and D. D. Xia, 2012: Interdecadal change of the connection between winter North Pacific Oscillation and summer precipitation in the Huaihe River valley. *Science China Earth Sciences*, **55**, 2049–2057.